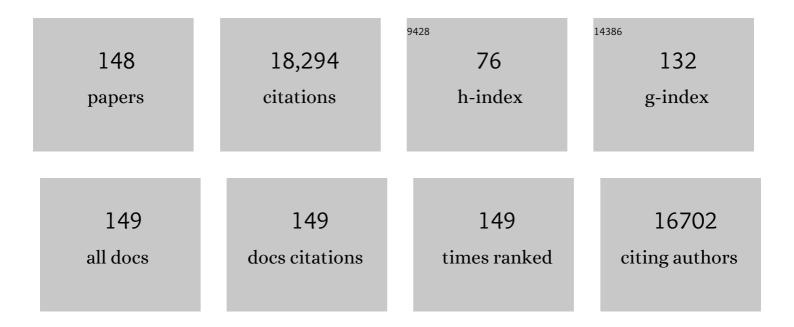
Xingzhong Yuan

List of Publications by Year in descending order

Source: https://exaly.com/author-pdf/586921/publications.pdf Version: 2024-02-01



#	Article	IF	CITATIONS
1	Photocatalytic removal of antibiotics by MOF-derived Ti3+- and oxygen vacancy-doped anatase/rutile TiO2 distributed in a carbon matrix. Chemical Engineering Journal, 2022, 427, 130945.	6.6	95
2	Tube wall delamination engineering induces photogenerated carrier separation to achieve photocatalytic performance improvement of tubular g-C3N4. Journal of Hazardous Materials, 2022, 424, 127177.	6.5	85
3	Defective polymeric carbon nitride: Fabrications, photocatalytic applications and perspectives. Chemical Engineering Journal, 2022, 427, 130991.	6.6	85
4	Carboxymethyl cellulose stabilized ferrous sulfide@extracellular polymeric substance for Cr(VI) removal: Characterization, performance, and mechanism. Journal of Hazardous Materials, 2022, 425, 127837.	6.5	35
5	Adsorption behaviors and mechanisms of Fe/Mg layered double hydroxide loaded on bentonite on Cd (II) and Pb (II) removal. Journal of Colloid and Interface Science, 2022, 612, 572-583.	5.0	71
6	Mechanistic insights of removing pollutant in adsorption and advanced oxidation processes by sludge biochar. Journal of Hazardous Materials, 2022, 430, 128375.	6.5	41
7	Manipulation of the halloysite clay nanotube lumen for environmental remediation: a review. Environmental Science: Nano, 2022, 9, 841-866.	2.2	11
8	Evaluating the remediation potential of MgFe2O4-montmorillonite and its co-application with biochar on heavy metal-contaminated soils. Chemosphere, 2022, 299, 134217.	4.2	11
9	Nearâ€Infrared Light Responsive TiO ₂ for Efficient Solar Energy Utilization. Advanced Functional Materials, 2022, 32, .	7.8	88
10	Application of functionalized layered double hydroxides for heavy metal removal: A review. Science of the Total Environment, 2022, 838, 155693.	3.9	33
11	Photocatalytic degradation of persistent organic pollutants by Co-Cl bond reinforced CoAl-LDH/Bi12O17Cl2 photocatalyst: mechanism and application prospect evaluation. Water Research, 2022, 219, 118558.	5.3	90
12	2D single- and few-layered MXenes: synthesis, applications and perspectives. Journal of Materials Chemistry A, 2022, 10, 13651-13672.	5.2	56
13	Singleâ€Atom Catalysts for Hydrogen Generation: Rational Design, Recent Advances, and Perspectives. Advanced Energy Materials, 2022, 12, .	10.2	42
14	Steering photo-excitons towards active sites: Intensified substrates affinity and spatial charge separation for photocatalytic molecular oxygen activation and pollutant removal. Chemical Engineering Journal, 2021, 408, 127334.	6.6	44
15	Photocatalytic degradation of tetracycline antibiotics using delafossite silver ferrite-based Z-scheme photocatalyst: Pathways and mechanism insight. Chemosphere, 2021, 270, 128651.	4.2	95
16	Core-shell Ag@nitrogen-doped carbon quantum dots modified BiVO4 nanosheets with enhanced photocatalytic performance under Vis-NIR light: Synergism of molecular oxygen activation and surface plasmon resonance. Chemical Engineering Journal, 2021, 410, 128336.	6.6	79
17	Burgeoning prospects of biochar and its composite in persulfate-advanced oxidation process. Journal of Hazardous Materials, 2021, 409, 124893.	6.5	122
18	Nanostructured covalent organic frameworks with elevated crystallization for (electro)photocatalysis and energy storage devices. Journal of Materials Science, 2021, 56, 13875-13924.	1.7	8

#	Article	IF	CITATIONS
19	Roles of sulfur-edge sites, metal-edge sites, terrace sites, and defects in metal sulfides for photocatalysis. Chem Catalysis, 2021, 1, 44-68.	2.9	83
20	Strategies to extend near-infrared light harvest of polymer carbon nitride photocatalysts. Coordination Chemistry Reviews, 2021, 439, 213947.	9.5	94
21	Recent advances on ZIF-8 composites for adsorption and photocatalytic wastewater pollutant removal: Fabrication, applications and perspective. Coordination Chemistry Reviews, 2021, 441, 213985.	9.5	180
22	Fabrication and regulation of vacancy-mediated bismuth oxyhalide towards photocatalytic application: Development status and tendency. Coordination Chemistry Reviews, 2021, 443, 214033.	9.5	90
23	Defect engineering in polymeric carbon nitride photocatalyst: Synthesis, properties and characterizations. Advances in Colloid and Interface Science, 2021, 296, 102523.	7.0	49
24	Recovery of CuO/C catalyst from spent anode material in battery to activate peroxymonosulfate for refractory organic contaminants degradation. Journal of Hazardous Materials, 2021, 420, 126552.	6.5	52
25	In-depth research on percarbonate expediting zero-valent iron corrosion for conditioning anaerobically digested sludge. Journal of Hazardous Materials, 2021, 419, 126389.	6.5	23
26	Strategic combination of nitrogen-doped carbon quantum dots and g-C3N4: Efficient photocatalytic peroxydisulfate for the degradation of tetracycline hydrochloride and mechanism insight. Separation and Purification Technology, 2021, 272, 118947.	3.9	65
27	In-situ construction of 2D/1D Bi2O2CO3 nanoflake/S-doped g-C3N4 hollow tube hierarchical heterostructure with enhanced visible-light photocatalytic activity. Chemical Engineering Journal, 2021, 426, 130767.	6.6	26
28	Selective graphene-like metal-free 2D nanomaterials and their composites for photocatalysis. Chemosphere, 2021, 284, 131254.	4.2	26
29	Recent advances in graphitic carbon nitride as a catalyst for heterogeneous Fenton-like reactions. Dalton Transactions, 2021, 50, 16887-16908.	1.6	23
30	Regeneration and reutilization of cathode materials from spent lithium-ion batteries. Chemical Engineering Journal, 2020, 383, 123089.	6.6	213
31	Stable self-assembly AgI/UiO-66(NH2) heterojunction as efficient visible-light responsive photocatalyst for tetracycline degradation and mechanism insight. Chemical Engineering Journal, 2020, 384, 123310.	6.6	150
32	Enhanced dewaterability of anaerobically digested sludge by in-situ free nitrous acid treatment. Water Research, 2020, 169, 115264.	5.3	73
33	New insight into modification of extracellular polymeric substances extracted from waste activated sludge by homogeneous Fe(II)/persulfate process. Chemosphere, 2020, 247, 125804.	4.2	24
34	Photocatalytic removal of antibiotics from natural water matrices and swine wastewater via Cu(I) coordinately polymeric carbon nitride framework. Chemical Engineering Journal, 2020, 392, 123638.	6.6	78
35	Advances in the application, toxicity and degradation of carbon nanomaterials in environment: A review. Environment International, 2020, 134, 105298.	4.8	241
36	A review on pyrolysis of protein-rich biomass: Nitrogen transformation. Bioresource Technology, 2020, 315, 123801.	4.8	131

#	Article	IF	CITATIONS
37	Core-shell structured cadmium sulfide nanocomposites for solar energy utilization. Advances in Colloid and Interface Science, 2020, 282, 102209.	7.0	36
38	Bioremediation of co-contaminated soil with heavy metals and pesticides: Influence factors, mechanisms and evaluation methods. Chemical Engineering Journal, 2020, 398, 125657.	6.6	235
39	Terephthalate acid decorated TiO2 for visible light driven photocatalysis mediated via ligand-to-metal charge transfer (LMCT). Colloids and Surfaces A: Physicochemical and Engineering Aspects, 2020, 603, 125188.	2.3	18
40	Peroxide/Zero-valent iron (Fe0) pretreatment for promoting dewaterability of anaerobically digested sludge: A mechanistic study. Journal of Hazardous Materials, 2020, 400, 123112.	6.5	49
41	Recent Progress on Fullerene-Based Materials: Synthesis, Properties, Modifications, and Photocatalytic Applications. Materials, 2020, 13, 2924.	1.3	29
42	Enhanced photocatalytic tetracycline degradation using N-CQDs/OV-BiOBr composites: Unraveling the complementary effects between N-CQDs and oxygen vacancy. Chemical Engineering Journal, 2020, 402, 126187.	6.6	131
43	Powerful combination of 2D g-C3N4 and 2D nanomaterials for photocatalysis: Recent advances. Chemical Engineering Journal, 2020, 390, 124475.	6.6	205
44	Fe(II) catalyzing sodium percarbonate facilitates the dewaterability of waste activated sludge: Performance, mechanism, and implication. Water Research, 2020, 174, 115626.	5.3	150
45	Mechanistic insights into heavy metals affinity in magnetic MnO2@Fe3O4/poly(m-phenylenediamine) coreâ^'shell adsorbent. Ecotoxicology and Environmental Safety, 2020, 192, 110326.	2.9	29
46	Integrating the (311) facet of MnO2 and the fuctional groups of poly(m-phenylenediamine) in core–shell MnO2@poly(m-phenylenediamine) adsorbent to remove Pb ions from water. Journal of Hazardous Materials, 2020, 389, 122154.	6.5	31
47	MXene Ti3C2 derived Z–scheme photocatalyst of graphene layers anchored TiO2/g–C3N4 for visible light photocatalytic degradation of refractory organic pollutants. Chemical Engineering Journal, 2020, 394, 124921.	6.6	181
48	Recent advances in titanium metal–organic frameworks and their derived materials: Features, fabrication, and photocatalytic applications. Chemical Engineering Journal, 2020, 395, 125080.	6.6	93
49	Biochar Facilitated Hydroxyapatite/Calcium Silicate Hydrate for Remediation of Heavy Metals Contaminated Soils. Water, Air, and Soil Pollution, 2020, 231, 1.	1.1	30
50	Physicochemical properties, metal availability and bacterial community structure in heavy metal-polluted soil remediated by montmorillonite-based amendments. Chemosphere, 2020, 261, 128010.	4.2	60
51	Ti ₃ C ₂ T _x MXene decorated black phosphorus nanosheets with improved visible-light photocatalytic activity: experimental and theoretical studies. Journal of Materials Chemistry A, 2020, 8, 5171-5185.	5.2	168
52	Stateâ€ofâ€ŧheâ€Art Advances and Challenges of Ironâ€Based Metal Organic Frameworks from Attractive Features, Synthesis to Multifunctional Applications. Small, 2019, 15, e1803088.	5.2	111
53	How does zero valent iron activating peroxydisulfate improve the dewatering of anaerobically digested sludge?. Water Research, 2019, 163, 114912.	5.3	124
54	Activated biochar with iron-loading and its application in removing Cr (VI) from aqueous solution. Colloids and Surfaces A: Physicochemical and Engineering Aspects, 2019, 579, 123642.	2.3	96

#	Article	IF	CITATIONS
55	Emergy and eco-exergy evaluation of wetland restoration based on the construction of a wetland landscape in the northwest Yunnan Plateau, China. Journal of Environmental Management, 2019, 252, 109499.	3.8	35
56	A real filed phytoremediation of multi-metals contaminated soils by selected hybrid sweet sorghum with high biomass and high accumulation ability. Chemosphere, 2019, 237, 124536.	4.2	39
57	Photocatalysis: Modulation of Bi ₂ MoO ₆ â€Based Materials for Photocatalytic Water Splitting and Environmental Application: a Critical Review (Small 23/2019). Small, 2019, 15, 1970122.	5.2	70
58	Synthesis and characterization of 2D/0D g-C3N4/CdS-nitrogen doped hollow carbon spheres (NHCs) composites with enhanced visible light photodegradation activity for antibiotic. Chemical Engineering Journal, 2019, 374, 479-493.	6.6	122
59	Modulation of Bi ₂ MoO ₆ â€Based Materials for Photocatalytic Water Splitting and Environmental Application: a Critical Review. Small, 2019, 15, e1901008.	5.2	179
60	Highly efficient removal of diclofenac sodium from medical wastewater by Mg/Al layered double hydroxide-poly(m-phenylenediamine) composite. Chemical Engineering Journal, 2019, 366, 83-91.	6.6	121
61	In-situ synthesis of 3D microsphere-like In2S3/InVO4 heterojunction with efficient photocatalytic activity for tetracycline degradation under visible light irradiation. Chemical Engineering Journal, 2019, 356, 371-381.	6.6	171
62	Electrical promotion of spatially photoinduced charge separation via interfacial-built-in quasi-alloying effect in hierarchical Zn2In2S5/Ti3C2(O, OH)x hybrids toward efficient photocatalytic hydrogen evolution and environmental remediation. Applied Catalysis B: Environmental, 2019, 245, 290-301.	10.8	229
63	Nitrogen doped carbon quantum dots promoted the construction of Z-scheme system with enhanced molecular oxygen activation ability. Journal of Colloid and Interface Science, 2019, 541, 123-132.	5.0	44
64	Adsorption behavior and mechanism of Mg/Fe layered double hydroxide with Fe3O4-carbon spheres on the removal of Pb(II) and Cu(II). Journal of Colloid and Interface Science, 2019, 536, 440-455.	5.0	207
65	Nitrogen self-doped g-C3N4 nanosheets with tunable band structures for enhanced photocatalytic tetracycline degradation. Journal of Colloid and Interface Science, 2019, 536, 17-29.	5.0	193
66	Facile synthesis of In2S3/UiO-66 composite with enhanced adsorption performance and photocatalytic activity for the removal of tetracycline under visible light irradiation. Journal of Colloid and Interface Science, 2019, 535, 444-457.	5.0	120
67	Simultaneously efficient adsorption and photocatalytic degradation of tetracycline by Fe-based MOFs. Journal of Colloid and Interface Science, 2018, 519, 273-284.	5.0	552
68	The migration and transformation behavior of heavy metals during co-liquefaction of municipal sewage sludge and lignocellulosic biomass. Bioresource Technology, 2018, 259, 156-163.	4.8	74
69	Effect of hydrothermal carbonization on storage process of woody pellets: Pellets' properties and aldehydes/ketones emission. Bioresource Technology, 2018, 260, 115-123.	4.8	16
70	Insight on the plasmonic Z-scheme mechanism underlying the highly efficient photocatalytic activity of silver molybdate/silver vanadate composite in rhodamine B degradation. Journal of Colloid and Interface Science, 2018, 530, 493-504.	5.0	40
71	Formation of quasi-core-shell In2S3/anatase TiO2@metallic Ti3C2Tx hybrids with favorable charge transfer channels for excellent visible-light-photocatalytic performance. Applied Catalysis B: Environmental, 2018, 233, 213-225.	10.8	297
72	Effective treatment of oily scum via catalytic wet persulfate oxidation process activated by Fe2+. Journal of Environmental Management, 2018, 217, 411-415.	3.8	20

#	Article	IF	CITATIONS
73	Effects of human activities and climate change on the reduction of visibility in Beijing over the past 36†years. Environment International, 2018, 116, 92-100.	4.8	39
74	In-situ synthesis of direct solid-state dual Z-scheme WO3/g-C3N4/Bi2O3 photocatalyst for the degradation of refractory pollutant. Applied Catalysis B: Environmental, 2018, 227, 376-385.	10.8	495
75	Near-infrared-driven Cr(<scp>vi</scp>) reduction in aqueous solution based on a MoS ₂ /Sb ₂ S ₃ photocatalyst. Catalysis Science and Technology, 2018, 8, 1545-1554.	2.1	41
76	Clayâ€Inspired MXeneâ€Based Electrochemical Devices and Photoâ€Electrocatalyst: Stateâ€ofâ€theâ€Art Progresses and Challenges. Advanced Materials, 2018, 30, e1704561.	11.1	431
77	Beneficial synergistic effect on bio-oil production from co-liquefaction of sewage sludge and lignocellulosic biomass. Bioresource Technology, 2018, 251, 49-56.	4.8	106
78	Quasi-polymeric construction of stable perovskite-type LaFeO3/g-C3N4 heterostructured photocatalyst for improved Z-scheme photocatalytic activity via solid p-n heterojunction interfacial effect. Journal of Hazardous Materials, 2018, 347, 412-422.	6.5	296
79	Construction of an all-solid-state Z-scheme photocatalyst based on graphite carbon nitride and its enhancement to catalytic activity. Environmental Science: Nano, 2018, 5, 599-615.	2.2	174
80	Recyclable zero-valent iron activating peroxymonosulfate synchronously combined with thermal treatment enhances sludge dewaterability by altering physicochemical and biological properties. Bioresource Technology, 2018, 262, 294-301.	4.8	115
81	Facile construction of novel direct solid-state Z-scheme AgI/BiOBr photocatalysts for highly effective removal of ciprofloxacin under visible light exposure: Mineralization efficiency and mechanisms. Journal of Colloid and Interface Science, 2018, 522, 82-94.	5.0	207
82	In situ surface transfer process of Cry1Ac protein on SiO2: The effect of biosurfactants for desorption. Journal of Hazardous Materials, 2018, 341, 150-158.	6.5	6
83	The effects of temperature and color value on hydrochars' properties in hydrothermal carbonization. Bioresource Technology, 2018, 249, 574-581.	4.8	71
84	Highly efficient photocatalysis toward tetracycline of nitrogen doped carbon quantum dots sensitized bismuth tungstate based on interfacial charge transfer. Journal of Colloid and Interface Science, 2018, 511, 296-306.	5.0	119
85	Implication of graphene oxide in Cd-contaminated soil: A case study of bacterial communities. Journal of Environmental Management, 2018, 205, 99-106.	3.8	75
86	Metal-free efficient photocatalyst for stable visible-light photocatalytic degradation of refractory pollutant. Applied Catalysis B: Environmental, 2018, 221, 715-725.	10.8	438
87	Molecular docking simulation on the interactions of laccase from Trametes versicolor with nonylphenol and octylphenol isomers. Bioprocess and Biosystems Engineering, 2018, 41, 331-343.	1.7	30
88	Highly efficient photocatalytic activity and mechanism of Yb3+/Tm3+ codoped In2S3 from ultraviolet to near infrared light towards chromium (VI) reduction and rhodamine B oxydative degradation. Applied Catalysis B: Environmental, 2018, 225, 8-21.	10.8	172
89	Immobilization of heavy metals in two contaminated soils using a modified magnesium silicate stabilizer. Environmental Science and Pollution Research, 2018, 25, 32562-32571.	2.7	31
90	A facile band alignment of polymeric carbon nitride isotype heterojunctions for enhanced photocatalytic tetracycline degradation. Environmental Science: Nano, 2018, 5, 2604-2617.	2.2	93

#	Article	IF	CITATIONS
91	Nitrogen doped carbon quantum dots mediated silver phosphate/bismuth vanadate Z-scheme photocatalyst for enhanced antibiotic degradation. Journal of Colloid and Interface Science, 2018, 529, 11-22.	5.0	81
92	Modified stannous sulfide nanoparticles with metal-organic framework: Toward efficient and enhanced photocatalytic reduction of chromium (VI) under visible light. Journal of Colloid and Interface Science, 2018, 530, 481-492.	5.0	89
93	Visible-light-driven removal of tetracycline antibiotics and reclamation of hydrogen energy from natural water matrices and wastewater by polymeric carbon nitride foam. Water Research, 2018, 144, 215-225.	5.3	481
94	Efficient visible-light driven photocatalyst, silver (meta)vanadate: Synthesis, morphology and modification. Chemical Engineering Journal, 2018, 352, 782-802.	6.6	65
95	Recent advances in synthesis, modification and photocatalytic applications of micro/nano-structured zinc indium sulfide. Chemical Engineering Journal, 2018, 354, 407-431.	6.6	171
96	Upgrading Sewage Sludge Liquefaction Bio-Oil by Microemulsification: The Effect of Ethanol as Polar Phase on Solubilization Performance and Fuel Properties. Energy & Fuels, 2017, 31, 1574-1582.	2.5	29
97	Plasmonic Bi nanoparticles and BiOCl sheets as cocatalyst deposited on perovskite-type ZnSn(OH) 6 microparticle with facet-oriented polyhedron for improved visible-light-driven photocatalysis. Applied Catalysis B: Environmental, 2017, 209, 543-553.	10.8	151
98	Phosphorus- and Sulfur-Codoped g-C ₃ N ₄ : Facile Preparation, Mechanism Insight, and Application as Efficient Photocatalyst for Tetracycline and Methyl Orange Degradation under Visible Light Irradiation. ACS Sustainable Chemistry and Engineering, 2017, 5, 5831-5841.	3.2	337
99	Doping of graphitic carbon nitride for photocatalysis: A review. Applied Catalysis B: Environmental, 2017, 217, 388-406.	10.8	1,194
100	Highly efficient visible-light-induced photoactivity of Z-scheme Ag ₂ CO ₃ /Ag/WO ₃ photocatalysts for organic pollutant degradation. Environmental Science: Nano, 2017, 4, 2175-2185.	2.2	121
101	Functionality of surfactants in waste-activated sludge treatment: A review. Science of the Total Environment, 2017, 609, 1433-1442.	3.9	100
102	Reply for comment on "Adsorptive removal of methylene blue by rhamnolipid-functionalized graphene oxide from wastewater― Water Research, 2017, 108, 464-465.	5.3	8
103	Photocatalytic Decontamination of Wastewater Containing Organic Dyes by Metal–Organic Frameworks and their Derivatives. ChemCatChem, 2017, 9, 41-64.	1.8	219
104	Facile synthesis of a novel full-spectrum-responsive Co2.67S4 nanoparticles for UV-, vis- and NIR-driven photocatalysis. Applied Catalysis B: Environmental, 2017, 202, 104-111.	10.8	102
105	Characteristics of Particulate Pollution (PM2.5 and PM10) and Their Spacescale-Dependent Relationships with Meteorological Elements in China. Sustainability, 2017, 9, 2330.	1.6	36
106	Facile synthesis of Sb2S3/ultrathin g-C3N4 sheets heterostructures embedded with g-C3N4 quantum dots with enhanced NIR-light photocatalytic performance. Applied Catalysis B: Environmental, 2016, 193, 36-46.	10.8	235
107	Enhanced adsorptive removal of p-nitrophenol from water by aluminum metal–organic framework/reduced graphene oxide composite. Scientific Reports, 2016, 6, 25638.	1.6	134
108	Risk assessment of heavy metals from combustion of pelletized municipal sewage sludge. Environmental Science and Pollution Research, 2016, 23, 3934-3942.	2.7	31

#	Article	IF	CITATIONS
109	Fast removal of tetracycline from wastewater by reduced graphene oxide prepared via microwave-assisted ethylenediamine–N,N'–disuccinic acid induction method. Environmental Science and Pollution Research, 2016, 23, 18657-18671.	2.7	37
110	Comprehensive assessment of eutrophication status based on Monte Carlo–triangular fuzzy numbers model: site study of Dongting Lake, Mid-South China. Environmental Earth Sciences, 2016, 75, 1.	1.3	30
111	Oneâ€pot selfâ€assembly and photoreduction synthesis of silver nanoparticleâ€decorated reduced graphene oxide/MILâ€125(Ti) photocatalyst with improved visible light photocatalytic activity. Applied Organometallic Chemistry, 2016, 30, 289-296.	1.7	149
112	A method for heavy metal exposure risk assessment to migratory herbivorous birds and identification of priority pollutants/areas in wetlands. Environmental Science and Pollution Research, 2016, 23, 11806-11813.	2.7	37
113	In situ synthesis of In2S3@MIL-125(Ti) core–shell microparticle for the removal of tetracycline from wastewater by integrated adsorption and visible-light-driven photocatalysis. Applied Catalysis B: Environmental, 2016, 186, 19-29.	10.8	538
114	Aggregate-based sub-CMC solubilization of n-alkanes by monorhamnolipid biosurfactant. New Journal of Chemistry, 2016, 40, 2028-2035.	1.4	28
115	Study on demetalization of sewage sludge by sequential extraction before liquefaction for the production of cleaner bio-oil and bio-char. Bioresource Technology, 2016, 200, 320-327.	4.8	58
116	Facile synthesis of amino-functionalized titanium metal-organic frameworks and their superior visible-light photocatalytic activity for Cr(VI) reduction. Journal of Hazardous Materials, 2015, 286, 187-194.	6.5	634
117	Complementary effects of torrefaction and co-pelletization: Energy consumption and characteristics of pellets. Bioresource Technology, 2015, 185, 254-262.	4.8	84
118	Novel visible light-induced g-C3N4–Sb2S3/Sb4O5Cl2 composite photocatalysts for efficient degradation of methyl orange. Catalysis Communications, 2015, 70, 17-20.	1.6	45
119	A facile hydrothermal method to synthesize Sb ₂ S ₃ /Sb ₄ O ₅ Cl ₂ composites with three-dimensional spherical structures. RSC Advances, 2015, 5, 53019-53024.	1.7	21
120	An integrated model for assessing heavy metal exposure risk to migratory birds in wetland ecosystem: A case study in Dongting Lake Wetland, China. Chemosphere, 2015, 135, 14-19.	4.2	93
121	Laccase behavior in the microenvironment of water core within a biosurfactant-based reversed micelles system rhamnolipid/n-hexanol/isooctane/water. Surface and Interface Analysis, 2015, 47, 491-497.	0.8	2
122	Facile synthesis of alumina-decorated multi-walled carbon nanotubes for simultaneous adsorption of cadmium ion and trichloroethylene. Chemical Engineering Journal, 2015, 273, 101-110.	6.6	129
123	Synthesis and applications of novel graphitic carbon nitride/metal-organic frameworks mesoporous photocatalyst for dyes removal. Applied Catalysis B: Environmental, 2015, 174-175, 445-454.	10.8	594
124	Three dimensional graphene based materials: Synthesis and applications from energy storage and conversion to electrochemical sensor and environmental remediation. Advances in Colloid and Interface Science, 2015, 221, 41-59.	7.0	242
125	Solvothermal synthesis of graphene/BiOCl _{0.75} Br _{0.25} microspheres with excellent visible-light photocatalytic activity. RSC Advances, 2015, 5, 33696-33704.	1.7	33
126	Photodeposition of metal sulfides on titanium metal–organic frameworks for excellent visible-light-driven photocatalytic Cr(<scp>vi</scp>) reduction. RSC Advances, 2015, 5, 32531-32535.	1.7	118

#	Article	IF	CITATIONS
127	The comparison of the migration and transformation behavior of heavy metals during pyrolysis and liquefaction of municipal sewage sludge, paper mill sludge, and slaughterhouse sludge. Bioresource Technology, 2015, 198, 16-22.	4.8	90
128	Facile preparation of an Ag/AgVO ₃ /BiOCl composite and its enhanced photocatalytic behavior for methylene blue degradation. RSC Advances, 2015, 5, 98184-98193.	1.7	55
129	One-step calcination method for synthesis of mesoporous g-C ₃ N ₄ /NiTiO ₃ heterostructure photocatalyst with improved visible light photoactivity. RSC Advances, 2015, 5, 95643-95648.	1.7	54
130	Chemical speciation, mobility and phyto-accessibility of heavy metals in fly ash and slag from combustion of pelletized municipal sewage sludge. Science of the Total Environment, 2015, 536, 774-783.	3.9	110
131	Aggregation of low-concentration dirhamnolipid biosurfactant in electrolyte solution. RSC Advances, 2015, 5, 88578-88582.	1.7	21
132	Distribution behavior and risk assessment of metals in bio-oils produced by liquefaction/pyrolysis of sewage sludge. Environmental Science and Pollution Research, 2015, 22, 18945-18955.	2.7	12
133	Aggregate-based sub-CMC solubilization of hexadecane by surfactants. RSC Advances, 2015, 5, 78142-78149.	1.7	25
134	Facile synthesis of CeO ₂ nanoparticle sensitized CdS nanorod photocatalyst with improved visible-light photocatalytic degradation of rhodamine B. RSC Advances, 2015, 5, 79556-79564.	1.7	77
135	A novel SnS2–MgFe2O4/reduced graphene oxide flower-like photocatalyst: Solvothermal synthesis, characterization and improved visible-light photocatalytic activity. Catalysis Communications, 2015, 61, 62-66.	1.6	99
136	Speciation and environmental risk assessment of heavy metal in bio-oil from liquefaction/pyrolysis of sewage sludge. Chemosphere, 2015, 120, 645-652.	4.2	100
137	Adsorptive removal of methylene blue by rhamnolipid-functionalized graphene oxide from wastewater. Water Research, 2014, 67, 330-344.	5.3	527
138	Removal of Basic Dye from Aqueous Solution using <i>Cinnamomum camphora</i> Sawdust: Kinetics, Isotherms, Thermodynamics, and Mass-Transfer Processes. Separation Science and Technology, 2014, 49, 2689-2699.	1.3	30
139	Co-pelletization of sewage sludge and biomass: The density and hardness of pellet. Bioresource Technology, 2014, 166, 435-443.	4.8	146
140	The migration and transformation behavior of heavy metals during the liquefaction process of sewage sludge. Bioresource Technology, 2014, 167, 144-150.	4.8	122
141	Magnetic separation and detection of a cellulase gene using core–shell nanoparticle probes towards a Q-PCR assay. Analytical Methods, 2012, 4, 2914.	1.3	2
142	Effects of surfactants on enzyme-containing reversed micellar system. Science China Chemistry, 2011, 54, 715-723.	4.2	15
143	Total concentrations and chemical speciation of heavy metals in liquefaction residues of sewage sludge. Bioresource Technology, 2011, 102, 4104-4110.	4.8	227
144	Effects of surfactants on ethanol production from rice straw by simultaneous saccharification and fermentation. , 2011, , .		1

#	Article	IF	CITATIONS
145	Effects of Surfactants Tween 80 and Rhamnolipid on the Extracellular Enzymes Amylase, Protease, CMCase and Xylanase of One Strain. , 2011, , .		4
146	Methane emissions from newly created marshes in the drawdown area of the Three Gorges Reservoir. Journal of Geophysical Research, 2009, 114, .	3.3	97
147	Adsorption of surfactants on a Pseudomonas aeruginosa strain and the effect on cell surface lypohydrophilic property. Applied Microbiology and Biotechnology, 2007, 76, 1189-1198.	1.7	55
148	Converting Waste Plastics into Liquid Fuel by Pyrolysis: Developments in China. , 2006, , 729-755.		12